Three Cations Intermixed InGaAs/InAlAs Quantum Well Structure and their Optical Gain Properties

Y. Chan, Michael C.Y. Chan and E. Herbert Li

University of Hong Kong, Department of Electrical and Electronic Engineering,
Pokfulam Road, Hong Kong.

ABSTRACT

Multiple cations intermixed $In_{0.53}Ga_{0.47}As/In_{0.52}Al_{0.48}As$ quantum well structure with 60 Å well width is investigated by using the expanded form of Fick's second law. It was found that a maximum compressive strain of 0.64% is obtained when annealing time reaches 3 hours at 812 °C in the indium sublattice. For a small interdiffusion, i.e. 1 to 1.5 hrs, the subband separation between the lowest heavy and light hole states is at its greatest. This is a major contribution to the band structure and averaged density of states, thus enhancement in optical gain up to 40% is obtained. For a large interdiffusion, i.e. up to 6 hrs., a large blue shift of the peak gain from 0.842 to 1.016eV is observed.

Keywords: III-V Semiconductor, Quantum Well, InGaAs/InAlAs, Interdiffusion, Optical gain.

1. INTRODUCTION

The *InGaAs/InAlAs* quantum well (QW) structures fabricated on *InP* substrate have a remarkable potential for application in long-haul and wide band width optical communication systems. The $In_{0.52}Al_{0.48}As$ barrier is lattice-matched to the substrate and changing the Group III sublattice composition in the *InGaAs* QW will give rise to different types of strain. The as-grown $In_{0.53}Ga_{0.47}As/In_{0.52}Al_{0.48}As$ QW has a bandgap transition energy of 0.84eV (wavelength λ=1.48μm), by the introduction of strain through the thermally induced QW composition intermixing technique[1], a tunable operation wavelength around 1.3μm can be obtained. This material system also offers high-speed modulation which is free from chirping[2], it therefore finds applications in electro-absorption modulators[3-4] and electro-optic waveguide switches[5] with switching capability up to multi-gigahertz. The *InGaAs/InAlAs* QW has many advantages over the quaternary *InGaAsP* materials. While the growth of high-quality quaternary materials such as *InGaAsP* remains a challenge, ternary *InGaAs/InAlAs* QW materials system on *InP* substrate is becoming a promising candidate. Apart from high material quality, good optical properties can be obtained by interdiffusion (otherwise known as intermixing) which changes the content of *In*, *Ga* and *Al* in the *InGaAs* well to a lattice-mismatched structure. This gives significant modification in the valence-band structure and hence improvement in the optical properties. The use of strained QW is known to be very important for the development of very low threshold current diode lasers.

The interdiffusion techniques are not only applicable in the tunability of device, enhancement in operation can also be obtained. In order to modify the device performance and to achieve tunability, a well-controlled interdiffusion technique is essential. By using impurity-induced enhanced intermixing, through ion implantation[6] or diffusion[7], and alternatively by impurity-free vacancy enhanced intermixing technique[8] through a masking process, selective area intermixing can be achieved planarly. These techniques not only have provided the wavelength tunability of devices[9], but it can also improve device performance[10] and are promising technologies for the integration of photonics IC's[11].

In this paper, we present a detailed theoretical analysis of the cation interdiffused *InGaAs/InAlAs* QWs. In section II, we will present the models for three species interdiffusion, induced change of concentration, in-plane strain and optical gain. In section III, a lattice matched as-grown structure is selected to demonstrate how the optical gain are affected by the technique of intermixing. Finally the conclusions are drawn.

2. MODELLING

2.1 Effects of disordering

A number of models have been presented for investigating interdiffusion which involves use of only one error function in approximating the compositional profiles. The QW studied here is *InGaAs/InAlAs*. In this system, multiple group III species (*In*, *Al* and *Ga*) become available as the interdiffusable constituent atoms which cannot necessarily be described by a single effective diffusion coefficients. In order to give a comprehensive interdiffused quantum well (DFQW) of this model, we have modeled the above system by the expanded form of Fick's second law:

$$\frac{\partial C_1}{\partial t} = \frac{\partial}{\partial z}\left(D_{11}\frac{\partial C_1}{\partial z}\right) + \frac{\partial}{\partial z}\left(D_{12}\frac{\partial C_2}{\partial z}\right) \tag{1}$$

$$\frac{\partial C_2}{\partial t} = \frac{\partial}{\partial z}\left(D_{21}\frac{\partial C_1}{\partial z}\right) + \frac{\partial}{\partial z}\left(D_{22}\frac{\partial C_2}{\partial z}\right) \tag{2}$$

where t is time, $C_1=C_1(z, t)$ and $C_2=C_2(z, t)$ are concentrations of *In*, and *Ga* respectively, D_{ij} (i,j=1,2) are the diffusion coefficients, D_{ii} is the diffusion rate of species i, that is, D_{11} and D_{22} are the diffusion rates of *In* and *Ga* respectively.and D_{ij} is the cross diffusion rate between species i and j such that D_{12} is the diffusion rates of *In-Ga* and D_{21} is that of *Ga-In*. The growth and hence the interdiffusion direction is along z and the center of the QW is defined at z=0. The diffusion coefficients are obtained by fitting the diffusion model to the measured concentration data by using least square to minimize the error and the values of Dij have been previously determined[12]. Then, by discretizing the diffusion equations into time and position steps, and by using the as-grown profile as the initial condition, the partial differential equations are solved. The solution to the finite difference method gives rise to the concentrations of the diffused species as a profile across the system normalized over the system. The concentration of Al, C_3 , is obtained by $C_3 = 1 - C_1 - C_2$ which is the stoichiometry boundary condition.

2.2 Effects of Strain

Lattice mismatch between thin well and thick barrier QW materials can be taken up by strain and results in a pseudomorphic QW such that an uniform lattice constant can be found through out the whole structure. This tetragonal deformation results in strain and which is, perpendicular to the hetero-interface. Assuming that the growth direction z is along <001>, the *InGaAs* well layer is subjected to a biaxial compressive in-plane strain parallel to x along <100> and to y along <010>, and a uniaxial shear strain parallel to z along <001>. The in-plane strain across the well will vary according to the composition of alloy concentration after interdiffusion. Hence the biaxial in-plane strain and uniaxial shear strain after interdiffusion, are given by :

$$\varepsilon_{xx} = \varepsilon_{yy} = \varepsilon(C_1, C_2) \tag{3}$$

$$\varepsilon_{zz} = -2[c_{12}(C_1, C_2)/c_{11}(C_1, C_2)]\varepsilon(C_1, C_2) \tag{4}$$

$$\varepsilon_{xy} = \varepsilon_{yz} = \varepsilon_{zx} = 0 \tag{5}$$

where $\varepsilon(C_1, C_2)$ is misfit factor between the well and the barrier and is defined to be negative for compressive strain, and $c_{ij}(C_1, C_2)$ are the elastic stiffness constants. The change in the bulk bandgap, $S_\perp(C_1, C_2)$, due to the hydrostatic component of strain is given by[13]:

$$S_\perp(C_1, C_2) = -2a(C_1, C_2)[1-c_{12}(C_1, C_2)/c_{11}(C_1, C_2)]\varepsilon(C_1, C_2) \tag{6}$$

where $a(C_1, C_2)$ is the hydrostatic deformation potential calculated from[13]:

$$a(C_1,C_2) = -\frac{1}{3}[c_{11}(C_1,C_2) + 2c_{12}(C_1,C_2)]\frac{dE_g(C_1,C_2)}{dP} \tag{7}$$

where dE_g/dP is the hydrostatic pressure coefficient of the lowest direct energy gap E_g The splitting energy, $S_{//}(C_1,C_2)$, between the heavy-hole (HH) and light-hole (LH) band edges induced by the shear component of strain is given by:

$$S_{//}(C_1,C_2) = -b(C_1,C_2)[1+2c_{12}(C_1,C_2)/c_{11}(C_1,C_2)]\varepsilon(C_1,C_2) \tag{8}$$

where $b(C_1,C_2)$ is the shear deformation potential. The coupling between LH and spin-off band gives rise to asymmetric HH to LH splitting[14], so that

$$S_{//HH}(C_1,C_2) = S_{//}(C_1,C_2) \tag{9}$$

$$S_{//LH}(C_1,C_2) = 1/2[S_{//}(C_1,C_2)+\Delta_o(C_1,C_2)]+1/2[9\{S_{//}(C_1,C_2)\}^2 + \{\Delta_o(C_1,C_2)\}^2 - 2S_{//}(C_1,C_2)\Delta_o(C_1,C_2)]^{1/2} \tag{10}$$

where $\Delta_o(C_1,C_2)$ is the spin-orbit splitting.

The QW confinement potential after the disordering process, $U_r(C_1,C_2)$, is obtained by modifying the unstrained potential profile after processing, $\Delta E_r(C_1,C_2)$, by the variable strain effects, and is given by:

$$U_r(C_1,C_2) = \Delta E_r(C_1,C_2) - S_{\perp r}(C_1,C_2) \pm S_{//r}(C_1,C_2) \tag{11}$$

where $S_{\perp r}(C_1,C_2) = Q_r S_{\perp}(C_1,C_2)$, the '+' and '-' signs represent the confined HH and LH profiles, respectively, and $S_{//c}(C_1,C_2) = 0$.

2.3 Sub-band-edge calculation

To calculate the electron and hole wave function in QW, the multiband effective mass theory is applied. For most III-V semiconductors such as *GaAs*-based materials, it is a good approximation that the conduction and valence bands are decoupled. A parabolic bands model and Luttinger-Kohn Hamiltonian with strain components are used for the conduction and valence bands respectively. The electron states near the conduction subband edge are assumed to be almost purely s-like and nondegenerate (excluding spin), while the hole states near the valence subband edge are almost purely p-like and four-fold degenerate (including spin). The envelope function scheme is adopted to describe the slowly varying (spatially extended) part of the wavefunction.

The wavefunctions of the electron and hole subband edge at the zone centre of Γ_6 valley symmetry can be calculated separately, using the Ben-Daniel and Duke model[15] by the one-dimensional Schrodinger-like equation, which is written as follows:

$$-\frac{\hbar^2}{2}\frac{d}{dz}\left[\frac{1}{m_r^*(z)}\frac{d\psi_{r\ell}(z)}{dz}\right] + U_r(z)\cdot\psi_{r\ell}(z) = E_{r\ell}\psi_{r\ell}(z) \tag{12}$$

where $\psi_{r\ell}(z)$ is the wavefunction of the ℓ^{th} subband for electrons($r = c\ell$) or holes ($r = v\ell$), respectively; $m_r^*(z)$ is the corresponding carrier effective mass in the z direction; $E_{r\ell}$ is the subband-edge energy. Equation (12) is solved numerically using a finite difference method with the above confinement profile. For valence band-mixing, it is much more complicated to solve in comparison with parabolic band model, thus preventing the diagonalization of the fourfold degenerate Luttinger Hamiltonian which can be solved using the finite difference method[16]. Alternatively, it can be solved

in the neighborhood of a high-symmetry zone centre (i.e., $k_{//}=0$) using approximation methods such as the one developed by Broido and Sham[18] using series expansions or the one by Chan[17] using an effective Hamiltonian.

2.4 Optical Gain

The propagation direction of the generated photon is parallel to the QW layers, and the gain spectrum is calculated by the density matrix approach. The gain spectrum due to the transition between the conduction subband p and the valence subband q is given by

$$g_{pq}(E) = \int dE' \sum_{p,q} \left[\frac{2\pi q^2 \hbar}{(2\pi)^2 n \varepsilon_0 c m_0^2 L_z E'} \cdot \int dk_{//} \left| \hat{e} \cdot P_{pq}(k_{//}) \right|^2 \cdot \right.$$
$$\left. \delta\left(E_p^e(k_{//}) - E_q^h(k_{//}) - E' \right) \times \left[f^e\left(E_p^e(k_{//}) \right) - f^h\left(E_q^h(k_{//}) \right) \right] \right] L(E - E'), \tag{13}$$

where q is the electric charge, n is the refractive index, ε_0 is the dielectric constant of the vacuum, c is the speed of light, L_z is the width of the quantum well, E is the photon energy, P_{pq} is the optical matrix element, $\hat{e}$ is a unit vector along the polarization direction of the optical electric field, and f^e and f^h are the Fermi distribution function for electron and hole in the conduction and valence subband, respectively. The spectral broadening of each transition is included, and the optical gain in a single quantum well structure is obtained with some spectral lineshape function over all transition energies E′. L(E – E′) is a Lorentzian line-broadening function and is given by

$$L(E - E') = \frac{1}{\pi} \frac{\hbar / \tau_{in}}{(E'-E)^2 + (\hbar / \tau_{in})^2} \tag{14}$$

where τ_{in} is the intraband relaxation time.

3. RESULTS AND DISCUSSION

The as-grown structure analyzed here is an $In_{0.53}Ga_{0.47}As/In_{0.52}Al_{0.48}As$ single quantum well, with as-grown well width L_z=60 Å. The as-grown QW is assumed to be fabricated on *InP* substrate with *InGaAs* in the well and *InAlAs* in the barrier forming a lattice matched QW structure.

The interdiffusion of the three cations (*In*, *Al* and *Ga*) are assumed to obey Fick's second law. Using the diffusion model with experimental data fitted interdiffusion coefficients, where $D_{In\text{-}In}$= 2.98, $D_{In\text{-}Ga}$= -4.01, $D_{Ga\text{-}In}$= 0.18 and $D_{Ga\text{-}Ga}$= 6.69 (in units of $10^{-18}cm^2s^{-1}$)[12], composition profiles can be obtained. Figure 1(a)-(c) show the variation of *In*, *Al* and *Ga* composition profiles in the DFQW with annealing time at a prescribed temperature 812 °C. In the initial stage of interdiffusion, there is an inverse process diffusion (diffusion from high concentration to low concentration) of *In* which diffused from barrier into the well. This is due to a much higher *Ga* diffusion rate so that *Ga* atoms take up all the vacancy in the barrier, thus suppressing the *In* diffusion out to the barrier[12]. As *InAs* has a larger lattice constant than those of *GaAs* and *AlAs*, compressive strain arises inside the well with increased *In* content. Likewise, as *Ga* has diffused out to the barrier, a tensile strain is built up near the hetero-interface. Fig. 2 shows the type of induced strain along the growth axis for a range of different extents of intermixing represented by diffusion time. As can be seen, the positive sign (tensile) strain is developed in the barrier while the negative sign (compressive) strain in the well. As a result of the non-uniform distribution of the *In*, *Al* and *Ga* atoms along the z direction, the strain changes from zero in the outer barrier to a maximum positive value at the interface and then to a minimum value at the center of the well. As t reaches 0.5 hours, two In concentration profile local peaks can be found at around z=±20Å, see Fig. 1(a), this gives rise to the double peaked magnitude compressive stress in the well, see Fig. 2. As interdiffusion proceeds further, intermixing has reached the center of well and the compressive strain has now increases in magnitude at the well center while the tensile strain also spreads out more into the barriers. The effective thickness of the *InGaAs* well should therefore be monitored in order to avoid dislocation. Maximum *In* concentration of 0.62 is obtained at the center of well as annealing time reaches 3 hours, this results in a corresponding 0.64% compressive strain. For annealing time exceeding 3 hours, the compressive strain relaxes in a gradual manner as shown in Fig. 3. For longer annealing time (t>6hrs), all three interdiffused composition

profiles become evenly distributed. This give rise to a reduction of strain in the well & barrier and thus relaxes the stress, as the constitution of the QW is now approaching that of an uniform *InAlGaAs* bulk material.

Optical gain is mainly dependent on the joint averaged density of states (DOS), Fermi occupation factor and optical matrix element[19]. The TE mode optical gain spectra of the DFQW with various extent of intermixing (indicated by diffusion time t) are showed in Fig. 4. The carrier density used in this calculation is fixed at 1.2×10^{12} cm^{-2}. In this figure, the peak gain energy can be seen to shift towards higher energies from λ=1.47 μm (0.842 eV) of an as-grown structure all the way to λ=1.22 μm (1.016 eV) of a DFQW (t=6 hrs). In the initial stage of interdiffusion (i.e. $t \leq 1.5$ hrs), an enhancement in peak gain magnitude up to 40% can be observed at t=1.0hr. This is because the difference between energy level of the ground state and the second state ΔE_{SUB}=58meV is large at the zone center and there is a reduction in the averaged DOS for the compressive-strained DFQW, both give rise to an improvement of the Fermi occupation factor. As the Fermi occupation factor, $f^{e}\left(E_{p}^{e}(k_{//})\right)-f^{h}\left(E_{q}^{h}(k_{//})\right)$, has a dominant role in the gain spectrum of the compressively-strained QW, a large enhancement in optical gain is obtained. In the case of the as-grown QW, it has a small ΔE_{SUB} (=39meV) and a large averaged DOS for its unstrained well, these result in a relatively lower optical gain. Thus, by employing QW intermixing, laser performance of *InGaAs/InAlAs* QW can be greatly enhanced. The peak gain magnitude will decrease as the extent of interdiffusion gets larger, because the QW structure is becoming more and more bulk-like.

4. CONCLUSION

In summary, we have presented the multiple cations interdiffusion of $In_{0.53}Ga_{0.47}As/In_{0.52}Al_{0.48}As$ single quantum well with well width of 60Å. The suppression of indium sublattice movement in the well exerts a significant influence on the compressive strain. At an annealing time of t = 3 hours, a maximum *In* concentration of 0.62 is found at the center of well which results in a compressive strain with 0.64% misfit. This creation of strain in the well through interdiffusion results in an enhancement of the optical gain by 40% as compared with the as-grown unstrained wells. This is because the compressive shear component of strain results in a reduced effective well width and a deepened potential well; thus contributing to the splitting of the heavy and light holes and resulting in an increase of the subband energy spacing. A large subband energy spacing of 58meV can be obtained at an annealing time of 1.0 hour, which is responsible for the substantial optical gain enhancement. The interdiffusion of the QW produce a blue shift of the peak gain energy, shifting from 0.842eV (λ=1.47μm) to 1.016eV (λ=1.22μm), which is useful in bandgap tuning applications. Interdiffusion in the $In_{0.52}Al_{0.48}As/In_{0.53}Ga_{0.47}As$ structure with initial annealing time between 1 and 1.5 hours will give the best laser operation, in terms of threshold current, optical gain and satisfactory differential gain.

5. ACKNOWLEDGEMENT

This paper is supported by the RGC earmarked grant of Hong Kong and the University of Hong Kong CRCG research grant.

6. REFERENCES

1. E.H.Li, Editor, *Quantum Well Intermixing for Photonics*, SPIE Milestone Series (to be published by SPIE, 1997)

2. K. Wakita, I. Kotaka, O. Mitomi, H. Asai and Y. Kawamura, "Observation of low-chirp modulation in InGaAs-InAlAs multiple-quantum well optical modulators inder 30 GHz", IEEE Photo. Technol. Lett., vol. 3, pp. 138-140, 1991.

3. T. Ido, H. Sano, D.J. Moss, S. Tanaka and A. Takai, "Strained InGaAs/InAlAs MQW electro-absorption modulators with large bandwidth and low driving VolHage", IEEE Photo. Technol. Lett., vol. 6, pp. 1207-1209,1994.

4. H.W. Wan, T.C. Chong and S.J. Chua, "Considerations for polarization insensitive optical switching and modulation using strained InGaAs/InAlAs quantum well structure", IEEE Photo. Technol. Lett., vol. 3 , pp. 730-732, 1991.

5. J.E. Zucker, K.L. Jones, G.R. Jacobovitz, B. Tell, K. Brown-Gobeler, T.Y. Chang, N.J. Sauer, M.D. Divino, M.Wegener and D.S. Chemla, "InGaAs - InAlAs quantum well intersecting waveguide switch operating at 1.55μm", IEEE Photo. Technol. Lett., vol. 2 , pp. 804-806, 1990.

6. D.G. Deppe and N. Holonyak, Jr., "Atom diffusion and impurity-induced layer disordering in quantum well III-V semiconductor heterostructure," J. Appl. Phys., vol. 64, pp. R93-R113, 1988.

7. I. Harrison, "Impurity-induced disordering in III-V multi-quantum well and superlattices," *J. Mat. Sci.: Mat. in Electron.*, vol. 4, pp. 1-28, 1993.

8 J.H. Marsh, "Quantum well intermixing," Semicond. Sci. Technol., vol. 8, pp. 1136-1155, 1993.

9. S. Burkner, J.D. Ralston, S. Weisser, J. Rosenzweig, E.C. Larkins, R.E. Sah and J. Fleissner "Wavelength tuning of high-speed InGaAs-GaAs-AlGaAs pseudomorphic MQW lasers via impurity-free interdiffusion," IEEE Photon. Technol. Lett., vol. 7, pp. 941-943, 1995.

10. W.C.H. Choy and E.H. Li, "The application of an interdiffused quantum well in a normally on electroabsorptive Fabry-Perot reflection modulator", IEEE J. Quantum Electron., vol. 33, no. 3, pp. 382-392, 1997.

11. E.S.Koteles, S. Charbonneau, P. Poole, J.J.He, M. Davies, M.Dion, G. Aers, Y. Feng, I.V. Mitchell and R.D. Goldberg, "Photonic integration using quantum well shape modification", Physics in Canada, pp.251-255, Sept/Oct 1996.

12. Y. Chan, W.C. Shiu, W.K. Tsui and E.H. Li, "Multiple cations interdiffusion in $In_{0.53}Ga_{0.47}As/In_{0.52}Al_{0.48}As$ quantum well", Proc. Material Research Society, vol.450, pp.337-382, 1997.

13. H. Asai and K. Oe, "Energy band-gap shift with elastic strain in $Ga_xIn_{1-x}O$ optixial layers on (001) GaAs substrates", J. Appl. Phys., vol. 54, pp. 2052-2056, 1993

14. R. People, "Indirect band gap of coherently strained Ge_xSi_{1-x} bulk alloys on <001> silicon substrates", Phys. Rev. B, vol. 32, pp. 1405-1408, 1985.

15. D.J. Ben-Daniel and C.B. Duke, "Space-charge effects on electron tunneling", Phys. Rev., vol. 152, pp. 683-692, 1966.

16. J. P. Loehr and J. Singh, "Theoretical- Studies of the Effect of strain on the Performance of Strained Quantum-Well Lasers Based on GaAs and InP Technology", IEEE J. Quantum Electron., vol. 27, pp. 708-716, 1991.

17. D. A. Broido and L. J. Sham, "Effective Masses of holes at GaAs-AlGaAs heterojunctions", Phy. Rev. B,

18. K.S.Chan, "The effects of the hole sub-band mixing on the energies and oscillator strengths of excitons in a quantum well", J. Phys. C, vol. 19, L125-L130, 1996.

19. S. Seki, T. Yamanaka, W. Lui, Y. Yoshikumi and K. Yokoyama, "Theoretical analysis of pure effects of strain and quantum confinement on differential gain in InGaAsP/InP strained layer quantum-well lasers", IEEE J. Quantum Electron., vol. 30, pp. 500-510, 1994.

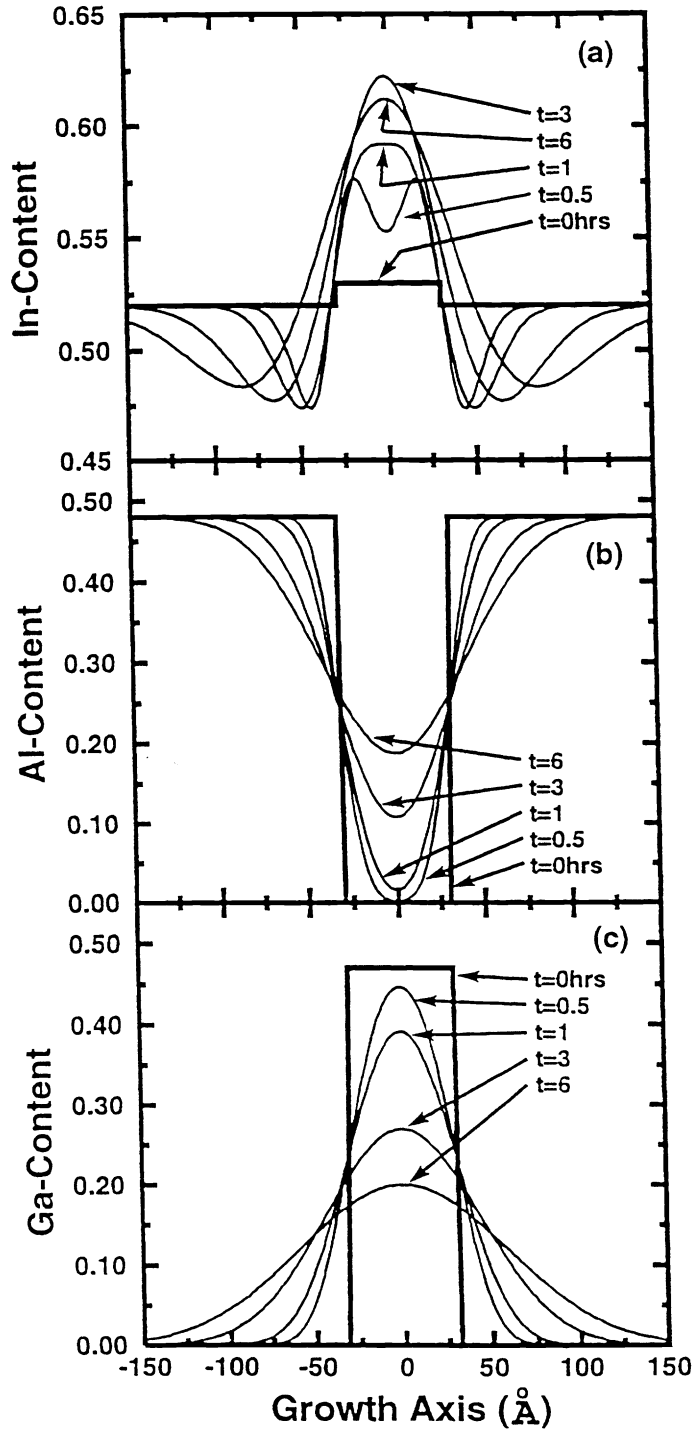

Figure 1. Three cations compositional profiles of $In_{0.53}Ga_{0.47}As/In_{0.52}Al_{0.48}As$ QW with as-grown well width of 60Å at 812 °C annealing temperature for as-grown (t=0) and several annealing time.

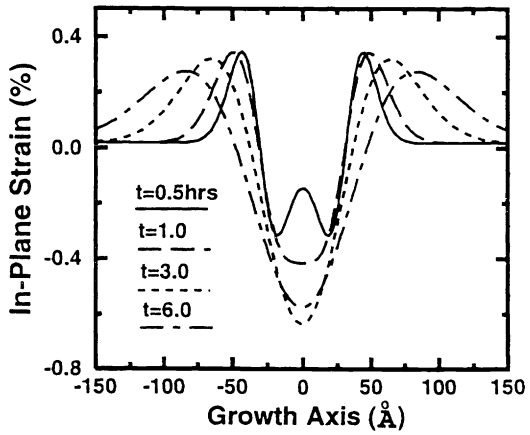

Figure 2. In-plane strain across the interdiffused QW for various annealing time.

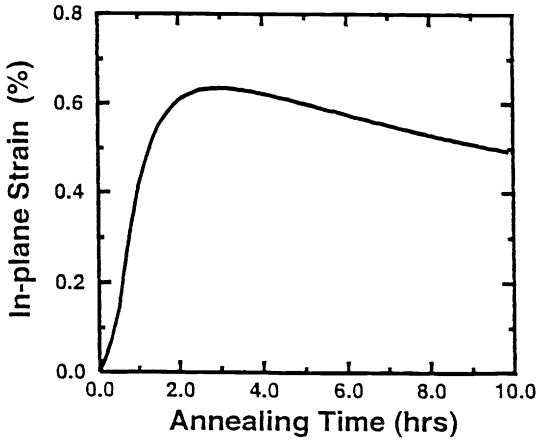

Figure 3. The in-plane compressive strain at the well centre for various annealing time.

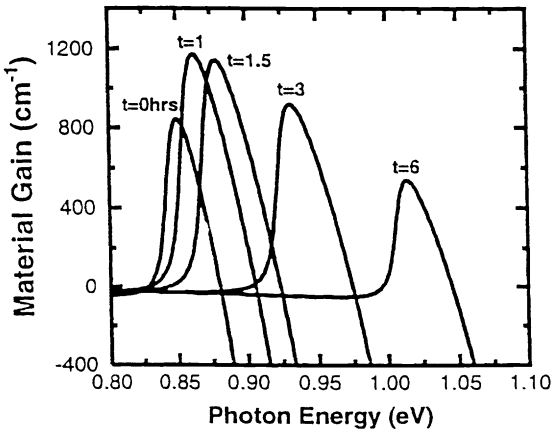

Figure 4. Optical gain spectra of $In_{0.53}Ga_{0.47}As/In_{0.52}Al_{0.48}As$ QW with as-grown well width of 60Å and at a fixed carrier injection level of $1.2x10^{12}cm^{-2}$ for various annealing time.